Available online at www.sciencedirect.com
SCIENCE DIRECT®
Biochemical and Biophysical Research Communications 330 (2005) 81–87
BBRC
www.elsevier.com/locate/ybbrc

A proteomics approach to identify changes in protein profiles in pre-cancerous colon ☆

Janice E. Drew [a,*], Garry J. Rucklidge [b], Gary Duncan [b], Awni Lufty [c], Andrew J. Farquharson [a], Martin D. Reid [b], Wendy R. Russell [a], Philip C. Morrice [a], John R. Arthur [a], Garry G. Duthie [a]

[a] *Cellular Integrity Division, Rowett Research Institute, Greenburn Road, Bucksburn, ABERDEEN, AB21 9SB Scotland, UK*
[b] *Proteomics Unit, Rowett Research Institute, Greenburn Road, Bucksburn, ABERDEEN, AB21 9SB Scotland, UK*
[c] *Dumfries Royal Infirmary, Dumfries, Scotland, UK*

Received 16 February 2005

Abstract

The development of colon cancer is characterised by alterations in multiple genetic and epigenetic pathways in colon tissue leading ultimately to deregulation of colon epithelial cells. Early detection is an important factor in decreasing colon cancer deaths. Proteomic techniques were used to identify potential early markers in colon tissue exhibiting pre-cancerous activity that may characterise pathological changes in a chemically induced colon cancer rat model. Protein profiles were assessed in soluble and insoluble fractions prepared from distal colon of rats treated with the colonotropic carcinogen, dimethylhydrazine. Alterations in protein profiles were associated with the presence of aberrant crypt foci, hyperplasia and dysplasia, microanatomical changes, and metabolic changes in rat colon. These changes may have a potential role in the identification of pre-pathological features preceding colon tumorigenesis.

Keywords: Proteomics; Colon cancer; Rat; Aberrant crypt foci; Prostaglandin

Colorectal cancer is the third most common cancer worldwide (excluding skin cancer) after lung and breast cancer [1]. Early detection significantly increases the chances of long-term survival [2]. However, bowel cancer is often detected at later stages when metastatic cancers have already progressed. Pathogenesis of colorectal cancer remains poorly understood. Although hereditary links to colorectal cancer development are well established, the majority of cases are sporadic with little or no evidence of hereditary factors [3]. The identification of novel markers that may predict the onset of pro-cancerous changes that predispose the colon to increased risk of tumorigenesis will be essential in reducing onset of this disease.

The protracted development (diagnosis is increasingly common between the ages of 50 and 70 years) and location of sporadic colorectal cancers in humans are problematic for conducting studies on the initiation and progression of this disease. Hence, a chemically induced colon cancer rat model is widely used to investigate the prevention and pathogenesis of this disease. The chemical carcinogen, dimethylhydrazine (DMH), produces pre-neoplastic aberrant crypt foci (ACF), and tumours in the colon of rodents [4]. Numerous studies have focused on ACF lesions in rodents and humans

☆ *Abbreviations:* ACF, aberrant crypt foci; AC, aberrant foci; CA-II, carbonate anhydrase II; CBR, carbonyl reductase; DMH, dimethylhydrazine; EIA, enzyme immunoassay; MDA, malondialdehyde; TBARS, thiobarbituric acid reactive substances; TPM, tropomyosin.

* Corresponding author. Fax: +44 1224 716629.
E-mail address: jed@rri.sari.ac.uk (J.E. Drew).

0006-291X/$ - see front matter © 2005 Elsevier Inc. All rights reserved.
doi:10.1016/j.bbrc.2005.02.125

(see review [5]). The molecular characteristics of ACF in rats show numerous similarities with those of human colon cancer. Analogous features typical of human colon cancer such as *K-ras* and *b-catenin* mutations [6,7], microsatellite instability [8], overexpression of COX2 [7] and cyclin D1 [8], and altered mucin secretion [9] have been identified in the rat model.

Colon cancer in humans is also associated with oxidative stress and related, increased indices of lipid peroxidation [10], and altered prostaglandin metabolism in colon [12,13]. These alterations in metabolism are also associated with colon pathologies linked to an increased risk of colon cancer (see reviews [14,15]). Enhanced lipid peroxidation can impact on cellular homeostasis and result in a wide range of concomitant changes in gene or protein expression (see reviews [16,17]) with potential pathological consequences. Alteration of homeostasis and analogous changes in oxidative stress and prostaglandin metabolism in colon tissue from DMH treated rats were assessed and indicators of a pre-cancerous disease state were established. Proteomics presents a relatively unexploited approach to identify associated molecular targets in soluble and insoluble protein extracts from colon tissue. MALDI-TOF-MS and peptide sequencing were used to identify proteins that are potentially indicative of the onset of cancer development.

Materials and methods

Animals and diets

Weanling male rats of the Rowett Hooded Lister strain were given a standard rat diet, ad libitum. The rats were given a single i.p. injection containing DMH (125 mg/kg body weight ~0.5 ml injection dissolved in sterile physiological saline). Control rats were injected with a similar volume of sterile physiological saline. Animal weights were recorded daily over the course of the experiment. The rats were anaesthetised with isoflurane 10 weeks after the injection. Colons were excised from the caecum at the ileo-caecal valve and rinsed with ice-cold sucrose/Tris (0.25 M sucrose/10 mM Tris, pH 7.4) solution to remove contents. Rectal segments were removed from the colon if present. Colon length measurements were recorded and proximal, transverse, and distal segments were snap-frozen separately for protein expression profiling and measurement of thiobarbituric acid reactive substances (TBARS) and microanatomical analysis. Alternatively, the colon segments were opened longitudinally and fixed flat in formalin for methylene blue staining and microscopical examination of lumenal epithelial abnormalities as described below.

Microscopical analysis of colon tissue

ACF and AC per ACF were scored in colons ($n = 6$ control group; $n = 8$ DMH treated group) at 10 weeks following the first carcinogen administration, essentially applying the procedure described by Bird [4]. Colons from corresponding sub-groups were killed at the same time point to provide tissues for biochemical and proteomic analyses. Immediately after the animals were killed, colons were removed, flushed with 0.9% NaCl solution, opened longitudinally, and fixed flat in 10% neutral buffered formalin (Sigma Chemical, UK). The colons were stained with methylene blue (0.1%) for 15 min. ACF and AC per ACF were scored and recorded using a Leica S4E microscope (Leica Microsystems Imaging Solutions, Cambridge, UK). Colons were examined microscopically and by immmunocytochemistry by a pathologist to confirm pre-cancerous changes in the colon of rats treated with DMH.

Cryostat sections (10 μm) were cut from each of the proximal, transverse, and distal colon regions, fixed in paraformaldehyde, and stained with toluidine blue. Microanatomical analysis was performed using a Leica DM IRB microscope and Leica QFluro imaging software (Leica Microsystems Imaging Solutions, Cambridge, UK). Well-orientated areas of colon sections were used to obtain measurements of crypt height, sub-mucosa, muscularis externa, and serosa depth (subserosa and serosa). Eight measurements were recorded for each parameter from transverse and distal sections obtained from each of the three rats per treatment group (a total of 24 measurements per parameter).

Biochemical analysis

Lipid peroxidation products were estimated in tissue homogenates as thiobarbituric acid reactive substances (TBARS) using HPLC and fluorimetric detection [18]. A Prostaglandin E metabolite EIA kit (Cayman Chemical) was used to assay PGE_2 metabolites according to the manufacturer's instructions. Colon segments were homogenised in Tris buffer (20 mM Tris–HCl, pH 7.4, 150 mM NaCl, 5 mM EDTA, 0.1 mM Na_3VO_4, leupeptin (4 μg/ml), toluene sulphonyl fluoride (60 μg/ml), and Triton X-100 (0.1%v/v)). Homogenates were derivatised immediately using the carbonate buffer supplied with the kit according to the manufacturer's instructions. The stable derivatives of PGE_2 metabolites formed were then quantified by EIA.

Proteomic analysis

Sample preparation. Although altered prostaglandin metabolism was measured throughout the colon, indicating disruption to optimal organ function in the pre-disease state, the distal colon was selected for proteomic analysis since this is the predominant location of ACF and tumour formation in human sporadic colon cancers and in the DMH treated rats. Protein was extracted from 0.5 cm colon segments by mild homogenisation and with a hand-held homogeniser in 200 μl of 40 mM Tris/HCl, pH 7.4, containing 3% DTT and protease inhibitor cocktail (Sigma), followed by brief sonication. The homogenate was centrifuged at 14,000 rpm on a bench-top centrifuge and the soluble proteins in the supernatant were decanted for 2D PAGE. The insoluble fraction was prepared by washing the remaining pellet with 40 mM Tris/HCl, pH 7.4. The pellet was then homogenised, sonicated, and centrifuged as above with 100 μl Bio-Rad 3 buffer (Bio-Rad sequential extraction kit). The supernatant containing the insoluble fraction was decanted for 2D PAGE. Estimation of protein concentration was performed using a Bio-Rad Bradford protein assay kit and using γ-globulin as standard.

2D PAGE conditions. The extracted protein fractions (300 μg) were loaded onto a Bio-Rad IPG strip (17 cm, pH 3–10) in 340 μl 7 M urea, 2 M thiourea, 4% Chaps, and 2% biolyte (Bio-Rad) 3% DTT buffer for separation of proteins in the first dimension. The second dimension SDS–PAGE step was run on an 18 × 18 cm linear SDS polyacrylamide gradient with a Bio-Rad Precision Plus Protein M_r standard at 200 V for 9.5 h prior to staining.

Protein staining and analysis. Colloidal Coomassie blue staining was performed as described by Anderson [19]. Gels ($n = 3$, each sample was run in triplicate, a total of 9 gels per treatment group) were then rinsed in deionised water, brushed to remove particulate Coomassie blue, and imaged on a Bio-Rad GS710 flat bed imager followed by image analysis using Bio-Rad PD Quest Version 7.1. The gel with the highest spot number and quality was selected as the match set standard. The PDQuest statistical analysis was performed on log

transformed matched set data from controls and DMH treated rats at 95% confidence interval.

Protein identification by nano LC/MS/MS

Samples from 2D PAGE gels were analysed using a nano LC system (LC Packings, Camberly, Surrey, UK) consisting of an 'Ultimate' nano LC system, pumping at 0.187 ml/min with a 625 splitter giving a column flow rate of 0.3 μl/min, a 'Famos' autosampler set to an injection volume of 5 μl, and a 'Switchos' microcolumn switching device. The nanocolumn was a C18 PepMap 100, 15 cm × 75 μm i.d., 3 μm, 100 Å (LC Packings). HPLC grade solvents were used: 2% acetonitrile and 0.1% formic acid (A), and 80% acetonitrile and 0.08% formic acid (B). The gradient started at 5% B, going to 50% B over 30 min, then ramping to 80% B over a further 2 min, and holding for 10 min. The system was equilibrated at 95% A for 9 min prior to injection of subsequent samples. The solvent used by the 'Switchos' is 0.1% formic acid. The switching device was switched on after 3 min and off after 58 min. The flow rate of the Switchos was 0.03 ml/min.

Mass spectrometry was performed using a Q-Trap (Applied Biosystems/MDS Sciex, Warrington, UK) triple quadrupole fitted with a nanospray ion source, where Q3 is operated as a linear ion trap (LIT). The nanospray needle voltage was set at 1850 V. Oxygen free nitrogen (OFN) was used as the curtain gas (set to 20) and the collision gas (set to high). In the survey scan mode, the mass range in Q1 was set to m/z 400–1200 with a scan rate of 4000 amu/s. The criterion for selection of ions for fragmentation (Q2) was ions of 10^5 cps (counts per second) or above. The collision energy was compound dependent (set to a maximum of 80 eV), and the charge state determination was 2–4. The trap fill time (Q3) was 250 ms and the scan rate was 1000 amu/s. The peptide profiles were analysed using the PROWL ProFound (Proteometrics, LLC, New York, USA, http://prowl.rockefeller.edu/) or Matrix Science (http://www.matrixscience.com/search_form_select.html) server-side tool. Profound and Mascot were used to match the mass spectra of peptide maps generated above against protein sequence databases (NCBInr, Swiss-Protnr or MSDB). Positive identities were at least 20% matched peptides covering at least 10% of the protein sequence.

Results

Microscopical analysis of colon tissue

Aberrant crypt foci of varying complexity (Fig. 1) were observed in the transverse and distal region of all DMH treated rats, but were absent in the proximal region (Table 1). No ACF were observed in the saline injected control rats (Table 1). The pathologist report confirmed hyperplasia and mild to moderate dysplasia in regions situated in the lower half of the colon (mid-transverse and distal) with over-expression of cyclin D1 in some lesions indicating pre-cancerous activity.

Examination of the cryostat sections of colon tissue revealed that each region (proximal, transverse, and distal) was microanatomically distinct and confirmed that comparable regions were obtained for all subsequent analyses. The geometric heterogeneity of the proximal region sections did not facilitate assessment of crypt heights and no significant differences were observed in the other parameters measured (Table 2). Significant increases were observed in muscularis mucosa depth in the transverse region, together with significant decreases in the depth of the sub-mucosa. Significant increases in crypt heights were observed in the distal colon of DMH treated animals (Table 2). The microanatomical changes recorded in the colon of DMH treated rats are indicative of altered morphology and are associated with the observed pre-cancerous activity.

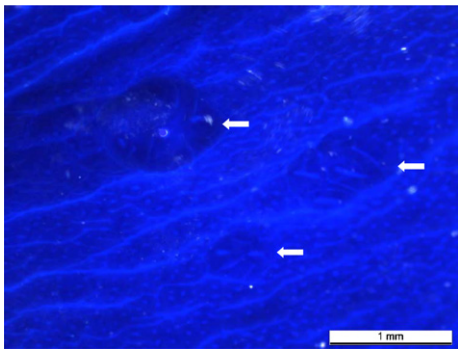

Fig. 1. Aberrant crypt foci in DMH treated rat colon. The lesions of varying complexity are marked by the white arrows and can be distinguished by the slightly elevated and irregularly shaped and elongated crypt openings.

Table 1
Aberrant crypt foci in control and DMH treated rats

Parameter	AC/foci			Total ACF/colon
	1–3	4–6	>7	
Control	0	0	0	0
DMH treatment	27.8 ± 4.4	23.6 ± 2.9	14.9 ± 1.6	66 ± 7.2

Values are means ± SE, $n = 6$ (control group), 8 (DMH treated group).

Effects of carcinogen on weight gain and colon metabolic homeostasis

Treatment with DMH did not affect final weights of the rats compared with control rats and there were no differences in colon length measurements (Table 2). Treatment with DMH was associated with altered indices of lipid peroxidation (TBARS) and increased prostaglandin levels in colon (Table 2).

Proteomics

Altered morphology, together with the biochemical changes observed in colon segments (Table 2), supports the use of a proteomics strategy to try and identify associated changes in protein profiles in adjacent colon segments. Pathogenesis of sporadic colon tumours and the occurrence of ACF in humans and in rats treated with DMH occur predominantly in the distal regions of the colon. Thus, 2D PAGE protein profiles of soluble and insoluble extracts were assessed from the distal

Table 2
Biochemical and microanatomical analysis of colon from control and DMH treated rats

Parameter	Control	DMH treatment
Colon length (cm)	19.3 ± 0.5	20.1 ± 0.5
Colon TBARS (nM MDA/mg protein)		
Proximal	2.8 ± 0.7	10.4 ± 5.6
Transverse	5.1 ± 2.8	18.0 ± 2.2***
Distal	33.6 ± 14.1	44.1 ± 11.9
Colon PGE2 metabolites (pg/mg colon tissue)		
Proximal	5.5 ± 0.3	6.4 ± 0.3***
Transverse	5.1 ± 0.4	6.9 ± 0.3**
Distal	5.7 ± 0.6	7.4 ± 0.4***
Crypt height (μm)		
Proximal	N/A	N/A
Transverse	666 ± 23	683 ± 13
Distal	425 ± 8	476 ± 11*
Sub-mucosa depth (μm)		
Proximal	59 ± 4	63 ± 4
Transverse	165 ± 16	121 ± 6**
Distal	130 ± 7	133 ± 7
Muscularis externa depth (μm)		
Proximal	224 ± 13	229 ± 9
Transverse	462 ± 20	575 ± 21*
Distal	240 ± 14	209 ± 8
Serosa depth (μm)		
Proximal	63 ± 3	68 ± 2
Transverse	102 ± 7	99 ± 5
Distal	71 ± 4	72 ± 3

Significant difference between control and DMH treated rats (*$p \leqslant 0.001$; **$p \leqslant 0.01$; ***$p \leqslant 0.05$; N/A parameter not assessed, see Results). Values are means ± SEM.

colon region. Around 200–500 spots were resolved from the insoluble and soluble fractions, respectively. Twenty-four spots from the soluble protein extract were selected as being differentially expressed ($p < 0.05$). Seven of the selected differentially expressed protein spots (Fig. 2) were identified from MALDI-TOF-MS spectra (Table 3) using the criteria outlined (see Protein identification by nano LC/MS/MS). Several factors influence the percentage of positive identifications obtained from the MALDI-TOF-MS spectra. Less stringent protein database search criteria can provide a greater number of protein identifications from the MALDI-TOF-MS spectra, but with a concomitant reduction in the confidence level of the protein identifications obtained. MS/MS analysis was deemed inappropriate if positive identification was not obtained from the MALDI-TOF-MS spectra. Identification of proteins from MALDI-TOF-MS spectra is also compromised by the occurrence of mixed populations in some protein spots on the 2D-gels. The soluble proteins identified included calreticulin, transgelin, carbonyl reductase, serotransferrin precursors, triosephosphate isomerase 1, creatine kinase mitochondrial 1, and carbonic anhydrase II (Table 3).

Four spots were selected for MALDI-TOF-MS analysis from the insoluble fractions on the basis of altered expression patterns (Fig. 3). These were all identified as being tropomyosin (M_r 29.7–31.4, pI 4.1 calculated from 2D PAGE). The mass spectra of the four spots revealed that spots labelled 1 (Fig. 3C) and 3 (Fig. 3D) were most similar. Likewise mass spectra of spots labelled 2 (Fig. 3C) and 4 (Fig. 3D) were more similar than the other

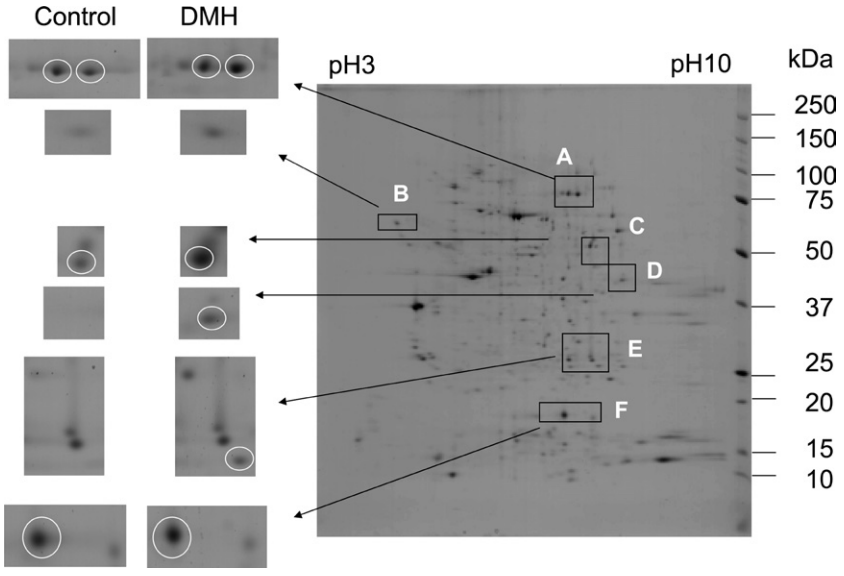

Fig. 2. A typical Coomassie stained gel showing 2D PAGE of soluble protein extracts from distal colon. Enlarged areas show significantly differentially expressed proteins ($p \leqslant 0.05$) extracted from control and DMH treated rats. (A) Serotransferrin precursor isoforms; (B) calreticulin; (C) carbonic anhydrase; (D) creatine kinase mitochondrial 1; (E) triosephosphate isomerase 1; and (F) transgelin.

Table 3
Proteins identified as being significantly elevated in DMH treated rat distal colon ($p \leqslant 0.05$)

Accession No.	Actual pI/M_w (kDa)	Protein identified	Calculated pI/M_w (kDa)
NP_071794.1	4.3/48.15	Calreticulin	4.6/54.21
NP_113737.1	8.9/22.5	Transgelin	7.4/19.64
NP_062043.1	8.5/30.85	Carbonyl reductase	7.6/31.37
P12346	7.0/78.57	Serotransferrin precursor	7.5/83.09
NP_075211.1	6.5/27.42	Triphosphate isomerase 1	7.9/27.46
XP_215806.1	8.9/47.34	Creatine kinase mitochondrial 1	8.3/44.94
P271396	9/29.27	Carbonic anhydrase II	7.7/55.59

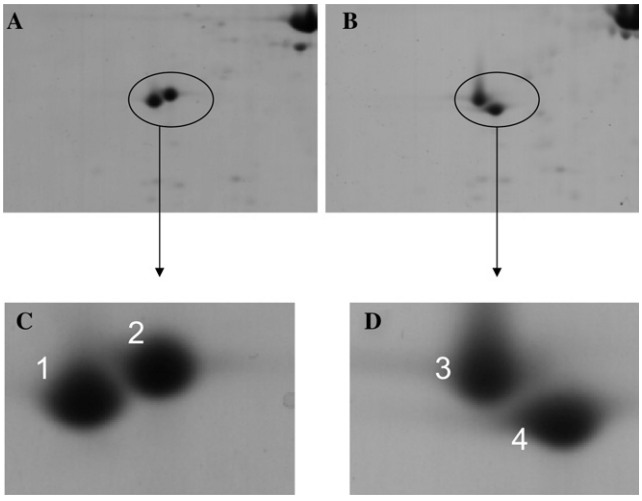

Fig. 3. Altered expression patterns of insoluble protein fractions. Spot patterns were from insoluble protein extracted from distal colon of (A) control and (B) DMH treated rats. (C,D) Enlarged images of the circled regions in (A,B), respectively. Mass spectra data identified all of these spots as tropomyosin.

two. Further analysis by peptide sequencing revealed that the spots represented different isomers of tropomyosin, potentially TPM1 and TPM2 (Table 4). Highest scores linked spots for TPM1 with spots 2 and 4 (Figs. 3C and D), and TPM2 with spots 1 and 3 (Figs. 3C and D). If the spots are manually aligned so that spots 1 (Fig. 3C) and 3 (Fig. 3D) match, then spots 2 and 4 exhibit an altered profile. Sequenced peptides identified the presence of splice variants of TPM1 and TPM2 (Table 4).

Table 4
Identified sequences of tropomyosin isomers showing altered expression patterns in DMH treated rat distal colon

Protein	Sequenced peptides
TPM1	LDKENAIDR*
	LEEEQQALQK
	DDAEADVASLNR
	VEEELD
	KLVILEGE
	EDKYEEEIK
TPM2	LDKENALDR*
	AEADVASLNR
	LVEEELDR
	EIQEIQLK
	LVIIESD
	AELEEELK
	KYEEEIKV

Alternative exon variants are marked *.

Discussion

Detection of morphological changes in colon tissue may be associated with several intestinal pathologies [20–23] and maintenance of structural morphology is essential for maintenance of optimal function of the gut mucosa [24–27]. Consequently, the enhanced lipid peroxidation, prostaglandin production in the bowel, and transverse and distal colon thickening measured in colon segments post-DMH treatment suggest a contribution to the development of clinical pathologies of the colon. Proteomic analysis of adjacent colon segments provides a useful tool to monitor biomarkers of genetic and epigenetic changes associated with altered homeostasis during the early stages of disease onset. Post-translational modifications that may be a unique feature of stressed tissues, such as phosphorylation, glycosylation, acetylation, and ubiquitination can also be investigated. Furthermore, there is the potential, as illustrated in this study, to identify altered expression of protein isomers. Specific protein isomers may prove important biomarkers of distinct stages of pathology or indicate particular stresses that lead to increased susceptibility to disease onset [28,29].

The proteins identified with altered expression are of potential importance in the metabolic changes observed in the pre-cancerous rat colon tissue. Calreticulin is a calcium binding protein of the cytoplasm, but may also be associated with nuclei and extracellular compartments. Anomalous migration is often observed in 2D PAGE (~60 kDa) due to its high negative charge (pI 4.7) (see Table 3). It has many potential functions in cell homeostasis including binding of hormone receptors to modify gene expression. It may be involved in alteration of MUC2 synthesis [30], which may be significant since MUC2 has been implicated in the development of colon cancer in the MUC2 knockout mouse [31]. Brunagel et al. [32] identified increased nuclear matrix protein calreticulin associated with human colon cancer.

Transgelin, a calponin-related protein characteristic of anti-inflammatory responses in both smooth muscle and non-muscle cells, was up-regulated in the soluble fractions from colon of rats treated with DMH. Counteracting inflammation is an important factor in preventing tumour-initiating events (see review [15]). Subsequent tumour progression leads to a loss of transgelin gene expression and down-regulation was identified in breast and colon cancer by ras-dependent and ras-independent mechanisms [33]. This supports a role in counteracting inflammatory pathways activated by DMH treatment and evidenced by increased prostaglandin production.

Carbonyl reductase (prostaglandin E2 9-reductase) belongs to the family of short chain dehydrogenases/reductases (SDR) [34]. Carbonyl reductases (CBRs) are NADPH-dependent, mostly monomeric, cytosolic enzymes with broad substrate specificity for many endogenous and xenobiotic carbonyl compounds. CBRs catalyse the reduction of endogenous prostaglandins, steroids, aliphatic aldehydes and ketones, and a wide variety of polycyclic aromatic hydrocarbon derived xenobiotic quinones. There is emerging evidence of the involvement of CBRs in a variety of cellular and molecular reactions associated with drug metabolism, detoxification, drug resistance, mutagenesis, and carcinogenesis. For example, dietary flavonoid compounds implicated in dietary prevention of colon cancer inhibit carbonyl reductase in rabbit heart [35]. CBR may play a role in metabolic processes linked to the altered levels of prostaglandin measured in DMH treated rats.

Serotransferrin precursors have a potential role in stimulating cell proliferation and may be colon cancer cell line growth factors [36]. Also tumours have an increased number of transferrin receptors. Serum levels of transferrin have been postulated as a marker of inflammatory bowel disease, together with C-reactive protein, also linked to colon cancer.

Triosephosphate isomerase 1 catalyses D-glyceraldehyde 3-phosphate to glycerone phosphate and plays a role in several metabolic pathways. Creatine kinase reversibly catalyses the transfer of phosphate between ATP and various phosphogens (e.g., creatine phosphate). Creatine kinase isoenzymes play a central role in energy transduction in tissues with large, fluctuating energy demands, such as skeletal muscle. Altered levels of triosephosphate isomerase 1and creatine kinase 10 weeks after DMH treatment may be a feature associated with altered metabolism predisposing the colon to pathological changes.

Carbonic anhydrase II (carbonate dehydratase II, CA-II) is a zinc metalloenzyme that assists rapid interconversion of carbon dioxide and water into carbonic acid, protons, and bicarbonate ions. CAII is a cytosolic form isozyme. Mammalian carbonic anhydrases occur in around 10 different forms depending upon the tissue or cellular location. Since this enzyme produces and uses protons and bicarbonate ions, carbonic anhydrase plays a key role in the regulation of pH and fluid balance in different parts of our body, such as the mucosal epithelium. Loss of optimal function in fluid absorption and digestion, and waste excretion can be symptoms of underlying colon pathology and are processes that are potentially disrupted in the pre-cancerous rat model used in this study.

The altered expression of tropomyosin isomers may be a significant factor in metabolic changes that result in the onset of disease since novel isoforms are associated with human colon cancer [29] and autoantibodies to particular isoforms are detected in ulcerative colitis [28]. At least 29 different isoforms of rat tropomyosin have been identified using RT-PCR strategies [37]. The tissue and cellular location and functions of the encoded proteins have yet to be fully elucidated.

The analysis of colon segments facilitated representation and examination of sub-populations of protein profiles from the distal colon. Cells from the epithelial layer together with underlying tissue were represented. This is important since the underlying tissues are intimately linked with the dynamic processes of proliferation, differentiation, and apoptosis that regulate the colon epithelia. Phenotypic and genotypic changes in cells underlying the epithelial layer have consequences for regulation of the colonic crypts and promotion of tumorigenesis.

Altered biochemical homeostasis was observed in the pre-cancerous colon as evidenced by elevations in prostaglandin levels and altered indices of oxidative stress (Table 2). Analogous changes are observed in human colon cancer [11–14]. Subsequent proteomic analysis identified associated protein biomarkers that may be altered during the disruption of homeostasis in colon tissue at the early stages of colon cancer development. The proteins identified in this study are linked to human colon pathologies, including cancer, providing further support for the use of the rat colon cancer model and further exploitation of proteomic approaches to investigate preventative colon cancer strategies.

Acknowledgments

We thank Mike Bromley for technical assistance (Dumfries Royal Infirmary) and Baukje de Roos (Rowett Research Institute) for helpful discussions. This work was supported by the Scottish Executive Environment and Rural Affairs Department (SEERAD).

References

[1] S. Bingham, E. Riboli, Diet and cancer—the European prospective investigation into cancer and nutrition, Nat. Rev. Cancer 4 (2004) 206–215.

[2] American Cancer Society. Available from: <www.cancer.org>.
[3] National Human Genome Research Institute. Available from: <www.genome.gov>.
[4] R.P. Bird, Observation and quantification of aberrant crypts in the murine colon treated with a colon carcinogen: preliminary findings, Cancer Lett. 37 (1987) 147–151.
[5] L. Cheng, M.D. Lai, Aberrant crypt foci as microscopic precursors of colorectal cancer, World J. Gastroenterol. 9 (2003) 2642–2649.
[6] N. Shivapurkar, Z. Tang, A. Ferreira, S. Nasim, C. Garett, O. Alabaster, Sequential-analysis of k-Ras mutations in aberrant crypt foci and colonic tumors induced by azoxymethane in Fischer-344 rats on high-risk diet, Carcinogenesis 15 (1994) 775–778.
[7] M. Takahashi, M. Mutoh, T. Kawamori, T. Sugimura, K. Wakabayashi, Altered expression of beta-catenin, inducible nitric oxide synthase and cyclooxygenase-2 in azoxymethane-induced rat colon carcinogenesis, Carcinogenesis 21 (2000) 1319–1327.
[8] F. Canzian, T. Ushijima, T. Serikawa, K. Wakabayashi, T. Sugimura, M. Nagao, Instability of microsatellites in rat colon tumors induced by heterocyclic amines, Cancer Res. 54 (1994) 6315–6317.
[9] R.K. Wali, S. Khare, M. Tretiakova, G. Cohen, Ursodeoxycholic acid and F(6)-D(3) inhibit aberrant crypt proliferation in the rat azoxymethane model of colon cancer: roles of cyclin D1 and E-cadherin, Cancer Epidemiol. Biomarkers Prev. 11 (2002) 1653–1662.
[10] J. Bara, M.-E. Forgue-Lafitte, N. Maurin, J.-F. Fléjou, A. Zimber, Abnormal expression of gastric mucin in human and rat aberrant crypt foci during colon carcinogenesis, Carcinogenesis Tumor Biol. 24 (2003) 109–115.
[11] E. Hietanen, H. Bartsch, J.C. Bereziat, A.M. Camus, S. McClinton, O. Eremin, L. Davidson, P. Boyle, Diet and oxidative stress in breast, colon and prostate cancer patients: a case-control study, Eur. J. Clin. Nutr. 48 (1994) 575–586.
[12] B. Rigas, I.S. Goldman, L. Levine, Altered eicosanoid levels in human colon cancer, J. Lab. Clin. Med. 122 (1993) 18–23.
[13] T. Kawamori, N. Uchiya, T. Sugimura, K. Wakabayashi, Enhancement of colon carcinogenesis by prostaglandin E-2 administration, Carcinogensis 24 (2003) 985–990.
[14] W.R. Bruce, A. Giacca, A. Medline, Possible mechanisms relating diet and risk of colon cancer, Cancer Epidemiol. Biomarkers Prev. 9 (2000) 1271–1279.
[15] L.M. Coussens, Z. Werb, Inflammationn and cancer, Nature 420 (2002) 860–867.
[16] R.G. Allen, M. Tresini, Oxidative stress and gene regulation, Free Rad. Biol. Med. 28 (2000) 463–499.
[17] K.J.A. Davies, Oxidative stress, antioxidant defenses, and damage removal, repair, and replacement systems, IUBMB Life 50 (2000) 279–289.
[18] C. Ramirez-Tortosa, Ø. Andersen, P.T. Gardner, S.G. Wood, P.C. Morrice, S.J. Duthie, A.R. Collins, G.G. Duthie, Anthocyanin-rich extract decreases indices of lipid peroxidation and DNA damage in vitamin E-depleted rats, Free Rad. Biol. Med. 31 (2001) 1033–1037.
[19] L. Anderson, Two Dimensional Electrophoresis—operation of the ISO-DALT System, Large Scale Biology Press, Rockville, MD, USA, 1991.
[20] G.W. Gardiner, R. Goldberg, D. Currie, D. Murray, Colonic carcinoma associated with an abnormal collagen table, Cancer 54 (1984) 2973–2977.
[21] M.F. Graham, A. Willey, J. Adams, Corticosteroids increase procollagen gene expression, synthesis and secretion by human intestinal smooth muscle, Gastroenterology 109 (1995) 1454–1461.
[22] G.J. Connett, J.S. Lucas, J.T. Atchley, J.J. Fairhurst, C.J. Rolles, Colonic wall thickening is related to age and not dose of high strength pancreain microspheres in children with cystic fibrosis, Eur. J. Gastroenterol. Hepatol. 11 (1999) 181–183.
[23] U. Gunther, D. Schuppan, M. Bauer, H. Matthes, A. Stallmach, A. Schmitt-Graff, E.O. Riecken, H. Herbst, Fibrogenesis and fibrolysis in collagenous colitis, Am. J. Pathol. 155 (1999) 493–503.
[24] A. Gledhill, F.M. Cole, Significance of basement membrane thickening in the human colon, Gut 25 (1984) 1058–1085.
[25] W.S. Hwang, J.K. Kelly, A disease of pericryptal fibroblast sheath, J. Pathol. 149 (1986) 33–40.
[26] J.R. Thiagarajah, P. Gourmelon, N.M. Griffiths, F. Lebrun, R.J. Naftalin, K.C. Pedley, Radiation induced cytochrome c release causes loss of rat colonic fluid absorption by damage to crypts and pericryptal myofibroblasts, Gut 47 (2000) 675–684.
[27] J.R. Thiagarajah, N.M. Griffiths, K.C. Pedley, R.J. Naftalin, Evidence for modulation of pericryptal sheath myofibroblasts in rat descending colon by transforming growth factor b and angiotensin II, Gastroenterology 2 (2002) 4–15.
[28] X. Geng, L. Biancone, H.H. Dai, J.J. Lin, N. Yoshizaki, A. Dasgupta, F. Pallone, K.M. Das, Tropomyosin isoforms in intestinal mucosa: production of autoantibodies to tropomyosin isoforms in ulcerative colitis, Gastroenterology 114 (1998) 912–922.
[29] J.L.-C. Lin, X. Geng, D. Bhattacharya, J.R. Yu, R.S. Reiter, B. Sastri, K.D. Glazier, Z.K. Mirza, K.K. Wang, P.S. Amenta, K.M. Das, J.J.C. Lin, Isolation and sequencing of a novel tropomyosin isoform preferentially associated with colon cancer, Gastroenterology 123 (2002) 152–162.
[30] D.J. McCool, Y. Okada, J.F. Forstner, G.G. Forstner, Roles of calreticulin and calnexin during mucin synthesis in LS180 and HT29/A1 human colonic adenocarcinoma cells, Biochem. J. 341 (1999) 593–600.
[31] A. Velcich, W. Yang, J. Heyer, A. Fragale, C. Nicholas, S. Viani, R. Kucherlapati, M. Lipkin, K. Yang, L. Augenlicht, Colorectal cancer in mice genetically deficient in the mucin Muc2, Science 295 (2002) 1726–1729.
[32] G. Brunagel, U. Shah, R.E. Schoen, R.H. Getzenberg, Identification of calreticulin as a nuclear matrix protein associated with human colon cancer, J. Cell. Biochem. 89 (2003) 238–243.
[33] J.M. Shields, K. Rogers-Graham, C.J. Der, Loss of transgelin in breast and colon tumors and in rie-1 cells by ras deregulation of gene expression through raf-independent pathways, J. Biol. Chem. 277 (2002) 9790–9799.
[34] G.L. Forrest, B. Gonzalez, Carbonyl reductase, Chem. Biol. Inter. 129 (2000) 21–40.
[35] Y. Imamura, T. Migita, Y. Uriu, M. Otagiri, T. Okawara, Inhibitory effects of flavonoids on rabbit heart carbonyl reductase, J Biochem. 127 (2000) 653–658.
[36] L.C. Yeoman, C.W. Wan, M.A. Zorbas, Transferrin and insulin enhance human colon tumor cell growth by differentiation class specific mechanisms, Oncol. Res. 8 (1996) 273–279.
[37] B.C. Cooley, G. Bergtrom, Multiple combinations of alternatively spliced exons in rat tropomyosin-alpha gene mRNA: evidence for 20 new isoforms in adult tissues and cultured cells, Arch. Biochem. Biophys. 390 (2001) 71–77.